Indian Journal of Chemical Technology
Vol. 25, November 2018, pp. 531-538

Study on the adsorption characteristics of aqueous caffeine solutions on macroporous resins with hydrogen-bonding interactions

Qingsheng Zhao[1], Jinhua Yin*[,1], Xu Wang[2], Deqing Du[3] & Qingguo Ye[1]

[*,1]College of Chemical Engineering, Qingdao University of Science & Technology, 266 042 Qingdao, China

[2] ZhangdianBorough of Quality and Technology Supervision, 255 000 Zibo, China

[3] Shandong Xinhua Pharmaceutical Co., Ltd, 255 000 Zibo, China

E-mail : yinjinhua@126.com

Received 17 January 2017; accepted 12 April 2018

The adsorption characteristics of caffeine on six macroporous resins have been investigated. The results show that the resin with hydroxyl groups (XDA-200) offer better adsorption/ desorption capacity than other resins, and its adsorption kinetics fit a pseudo- second-order model. The adsorption process is a type of fast adsorption, and multiple adsorption mechanisms controlled the rate of adsorption. The isothermal equilibrium curve of caffeine adsorbed onto XDA-200 show a good fit to the Freundlich model, and thermodynamics tests show that the process is exothermic and spontaneous. The absolute value of enthalpy is 14.347 kJ/mol, which is in the range of the adsorption enthalpy related to hydrogen-bonding interactions. XPS and FTIR analyses also verify the existence of hydrogen-bonding interactions.

Keywords: Macroporous resin, Caffeine, Adsorption isotherm, Adsorption kinetics, Hydrogen-bonding interaction

In the past decades, there has been an increasing interest in tea, because of its potential health benefits[1]. Tea possess various biological, physiological and pharmaceutical effects, such as antioxidant, anticancer, and antibacterial effects[2, 3]. Caffeine is a type of xanthine alkaloid compound (Fig.1) and an important ingredient of tea, which can improve the excitability of the nervous system, is an antipyretic and analgesic, and has a good protection effect on heart and cerebral vessels. Moreover, caffeine is also the most widely used psychotropic drug in the word and has attracted much attention because of its special efficacy[4-6]. However, long-term intake or large doses of caffeine can cause damage to the human body in the form of sleep deprivation, increased risk of cardiovascular disease and miscarriages, reduced fertility rates, and increased seizure frequency and aggravated seizures[7,8]. So far, many technologies have been developed for the extraction of caffeine from tea, such as organic solvent extraction[9] and supercritical fluid extraction[10]. Of all the methods for the extraction and purification of caffeine, solvent extractionis a traditional and mature technique. However, organic solvent extraction has various disadvantages, such as requiring relatively large quantities of solvents, toxic solvents, and long extraction times[11]. Moreover, other methods are not only relatively complex but also consume large amounts of energy. Hence, with the increasing awareness of problems of environmental pollution, it is urgent to develop easy, effective, low toxicity and economic methods.

In recent years, growing attention has been paid to macroporous resins due to their excellent performance in the separation and purification of pharmaceutical and natural products[12, 13]. Compared with other adsorbents, macroporous resins are more applicable because of their favorable physicochemical stability, large adsorption capacity, high adsorption selectivity, and structural diversity[14].

To find the appropriate adsorption resin and separation methods, six kinds of resins with different specific surface areas, pore diameters, and functional groups were used in this study to investigate the adsorption and desorption properties of caffeine. In this paper, we determined the optimal resin of the six and furthermore investigated the effect of temperature, the adsorption kinetics, and the thermodynamics. In addition, XPS survey scans and FTIR analyses were used to monitor the surface electronic state and chemical changes, respectively, in the optimal resin before and after adsorption. The

results indicated that the adsorption capacity of the selected resin was remarkable and much higher than those of commonly used adsorbents.

Experimental Section

Materials and reagents

All the macroporous resins with a styrene-divinyl benzene structure (LX-17, LX-18, D101, D301, XDA-1, XDA-200) used in our study were supplied by Xi'an Sunresin Technology Co., Ltd. (Shaanxi, China). Analytical-grade caffeine was supplied by Shandong Xinhua Pharmaceutical Co., Ltd. (China). Analytical-grade ethanol, hydrochloric acid, and sodium hydroxide were purchased from YantaiSanheChemical Reagent Co., Ltd. (Shandong, China).

Pretreatment of resins

Physical characteristics of the macroporous resins are given in Table 1. To remove impurities, including residual porogenic agents and monomers produced during synthesis, all the resins in the wet form were first pretreated with ethanol and then thoroughly washed with deionized water. Subsequently, all the resins were regenerated by 3% NaOH and HCl. Finally, they were washed with deionized water to achieve a neutral *p*H and dried in a vacuum oven at 323K to a constant weight.

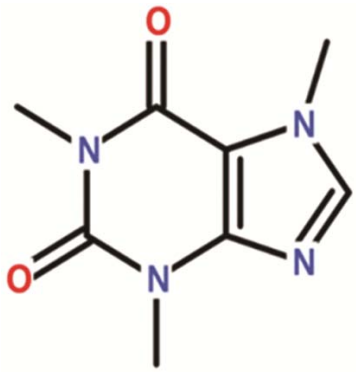

Fig. 1 — Molecular structure of caffeine

Table 1 — Physical characteristics of the macroporous resins.

Resin code	Polarity	Functional group	Particle size(mm)	Surface area(m^2/g)	Average pore size(nm)
LX-17	strong-polar	-	0.315-1.25	≥460	-
LX-18	non-polar	none	0.2-0.7	≥1100	-
D101	non-polar	none	0.2-0.3	754	5.18
D301	polar	$-N(CH_3)_2$	0.400-0.700	>1100	13-14
XDA-1	strong-polar	-OH	0.315-1.25	>1000	7.44
XDA-200	weak-polar	-0H	0.4-1.25	1000	20

Static adsorption and desorption Tests

Static adsorption/desorption experiments were carried out as follows. First, 2.0 g dry resin and 50 mL caffeine solution with a concentration of 10 mg/mL were added into 250 mL conical flasks with stoppers. Then, the flasks were continually shaken by a constant-temperature water bath oscillator under 150 rpm for 12 h, and the temperature was set at 298 K. After adsorption equilibrium was reached, the final concentrations of caffeine in the solutions were determined by GC. Furthermore, after adsorption equilibrium was reached, static desorption experiments were carried out as follows. First, the resins were filtrated from the solution and then adequately washed by deionized water. Subsequently, 50 mL ethanol-water (80%V/V) was added to the 250 mL conical flasks containing the adsorption-laden resins. The flasks were continually shaken by a constant-temperature water bath oscillator under 150 rpm for 12 h at 333K. Then, the corresponding caffeine contents of the desorbents were determined by GC. To determine the optimal resin of the six, the adsorption capacity, adsorption rate, and desorption rate was preliminarily evaluated, and the equations used in the study were as follows:

$$q_e = \frac{(C_o - C_e)V}{M}$$

$$\beta_1 = \frac{(C_0 - C_e)}{C_0} \times 100\%$$

$$\beta_2 = \frac{C}{C_0 - C_e} \times 100\%$$

where q_e is the equilibrium adsorption capacity of caffeine, mg/g; β_1 is the adsorption rate of caffeine, %; β_2 is the desorption rate of caffeine, %; C_0 and C_e are the initial and equilibrium concentrations of the caffeine solution, mg/mL; C is the concentration of the desorption solution, mg/mL; V is the volume of the caffeine solution used in the experiment, mL; and W is the dry resin weight, g.

Adsorption isotherms on the selected resin

The equilibrium adsorption of caffeine onto XDA-200 in aqueous solution was studied at 293, 303, and 313K. Approximately 2.0 g dry resin was mixed with 50mL standard caffeine solution, and the initial concentrations of the aqueous caffeine solutions were set at 2-16 mg/mL, with 2 mg/mL intervals. Subsequently, the flasks with stoppers were shaken

for 12 h under 150 rpm, and the final concentrations of caffeine in the solutions were determined by GC.

Currently, the Langmuir and Freundlich isotherms are often adopted to describe adsorption process[15-17].

The Langmuir isotherm can be expressed as:

$$q_e = \frac{q_{max} K_L C_e}{1 + K_L C_e}$$

The Freundlich isotherm can be given as:

$$q_e = K_F C_e^n$$

Where C_e is the equilibrium concentration, mg/L; q_e is the amount of caffeine adsorbed at equilibrium, mg/g; q_m is the maximum adsorption capacity of caffeine on the adsorbent, mg/g; q_e is the equilibrium adsorption capacity of caffeine on the adsorbent, mg/g; K_L is the Langmuir constant, and the value of K_L indicates whether the isotherm is favorable; K_F is a characteristic parameter and can be used as an indicator of adsorption capacity; and n refers to the adsorption intensity and is usually used as an indicator of whether the adsorbent/adsorbate system is favorable.

Adsorption thermodynamics on the selected resin

To account for the adsorption process of caffeine on XDA-200, various thermodynamic parameters were calculated in this study. The corresponding values of △G, △H, and △S are presented in Table 4. Thermodynamic parameters, such as △G, △H, and △S, associated with the adsorption process can be estimated using the following equations.

The Van't-Hoff equation can be expressed as:

$$\ln K_F = -\frac{\Delta H}{RT} + A$$

where △H is the adsorption enthalpy, kJ/mol; R is the ideal gas constant, 8.314J/(mol·K); T is the absolute temperature, K; K_F is the Freundlich constant; and A is a constant.

The Gibbs free energy can be calculated as:

$$\Delta \mathrm{G} = -\mathrm{RT}\ln K_F$$

where △G is the adsorption Gibbs free energy, kJ/mol; R is the ideal gas constant, 8.314J/(mol·K); T is the absolute temperature, K; and K_F is the Freundlich constant.

The adsorption entropy can be calculated using the Gibbs-Helmholtz equation:

$$\Delta S = \frac{\Delta H - \Delta G}{T}$$

where △S is the adsorption entropy.

Adsorption kinetics on the selected resin

The adsorption kinetics curves of caffeine on the optimal resin at different temperatures (20, 30, 40 °C) were obtained as follows.The pretreated resin (equal to 2.0 g dry resin) and 100 mL caffeine solution with an initial concentration of 10 mg/mL were added into a 250 mL conical flasks with lids. Subsequently, the flasks were continually shaken by a constant-temperature water bath oscillator under 150 rpm until the adsorption equilibrium was reached. In this process, 0.1 mL of standard solution was sampled as soon as possible at different time intervals to analyze the residual concentration by GC. The adsorption capacity at contact time t was calculated by the following equation:

$$\mathrm{q_t} = \frac{(\mathrm{C_0} - \mathrm{C_t})\mathrm{V}}{\mathrm{M}}$$

where C_0 and C_t are the concentrations of caffeine at the initial time and contact time t, respectively, and q_t is the adsorption capacity at contact time t.

To better illustrate the adsorption mechanism, the following kinetics models were employed to describe the adsorption process: pseudo-first-order, pseudo-second-order and particle diffusion kinetics models. The parameters fit by the equations are shown in Table 5.

The pseudo-first-order kinetics model can be expressed as:

$$\ln(q_e - q_t) = -k_1 t + ln q_e$$

The pseudo-second-order kinetics modelcan be expressed as:

$$\frac{1}{\mathrm{q_t}} = \frac{1}{\mathrm{k_2 q_e^2}} \cdot \frac{1}{\mathrm{t}} + \frac{1}{\mathrm{q_e}}$$

The particle diffusion kinetics model can be expressed as:

$$q_t = k_d \cdot t^{\frac{1}{2}} + C$$

where k_1, k_2 and k_d are the first-order, second-order and intra-particle rate constants, respectively;q_e and $q_t$are the amount of caffeine adsorbed onto XDA-200 at equilibrium and at time t, respectively; and the value of C indicates the thickness of the boundary layer, wherethe resistance to external mass transfer increases as the intercept increases.

GC Analysis

GC analysis was performed on a Shimadzu GC-14C series GC system (Shimadzu Instrument Co., Ltd, Suzhou, China) equipped with an FID detector. In this study, all concentrations of the caffeine solutions before and after adsorption were determined by GC, and phenacetin was selected as the internal standard. The capillary column used in the study is a PEG-20M column (30 m×0.25 mm×0.25 μm, Lanzhou Institute of Chemical Physics, Gansu, China)with a Se-30 stationary phase. The column temperature, injection temperature, and detector temperature were kept at 220, 250, and 250 °C, respectively. The flow rate of nitrogen, hydrogen, and air were 5, 30, and 100 mL/min, respectively. The split ratio was 1:20, and the injection volume was 0.5 μL. The initial concentrations of the standard caffeine solutions were set at 2-16 mg/mL, with 2 mg/mL intervals. First, 1 mL of the standard caffeine solutions with different known concentrations were mixed with the 0.5% phenacetin solution($m_{phenacetin}/m_{ethanol}$) in equal volume. Then, the peak area ratios of caffeine to phenacetin were separately determined under the same GC conditions. A good linear relationship was obtained over the range of 2-16 mg/mL, and the regression line for caffeine was Y=0.05709+0.11498X (R^2=0.9991), where Y is the peak area ratio of caffeine to phenacetin and X is the concentration of caffeine.

Results and Discussion

Static adsorption and desorption tests

The adsorption and desorption capacities of caffeine on the six resins are shown in Table 2.

As shown in Table 2, XDA-200, XDA-1, and LX-18 showed the strongest adsorption capacities (222.75, 209.01, and 156.22 mg/g dry resin, respectively), followed by D101 (125.99 mg/g dry resin). However, LX-17 and D301 possessed the lowest adsorption capacities (65.4 and 90.42, respectively). In addition, when XDA-200, XDA-1, and LX-18 were used, the highest adsorption ratios of caffeine were observed (89.10%, 83.60%, and 62.48%, respectively). However, the desorption ratios of caffeine for the six resins in 80% ethanol solution decreased in the order of XDA-200> D301 > LX-18 > XDA-1> LX-17 > D101. The desorption capacity of XDA-1 was rather low, probably due to the polar resin possessing a strong affinity for caffeine via its surface electrical properties and hydrogen bonding interactions; thus, the desorption capacity of caffeine on XDA-1 was not notable[18]. XDA-200 exhibited a higher adsorption capacity, mainly because the polarity of caffeine is relatively weak, and its polarity was weakly polar or nonpolar;moreover, the polarity of XDA-200 is weak. According to the rule “like dissolve like”, the resin with lower polarity exhibited better adsorption of lowerpolarity and non-polar substances. Furthermore, XDA-200 had a higher specific surface area, which provided more active adsorption sites. Additionally, compared with the other resins, XDA-200 had a larger average pore diameter, reducing the steric hindrance and ensuringthe flow of caffeine molecules from the solution to the pore channels. Hence, XDA-200 was chosen for the following adsorption thermodynamics and kinetics studies.

Adsorption Isotherms on the selected resin

Fig. 2 shows the adsorption isotherm of caffeine on XDA-200, and the caffeine uptake increased with an

Table 2 — dsorption capacity, desorption capacity and desorption ratio of the different resins.

Macroporous resin	q_e/mg.g^{-1}	β_1/%	β_2/%
LX-17	65.40	26.16	29.81
LX-18	156.22	62.48	55.43
D101	125.99	50.4	27.64
D301	90.42	36.17	67.89
XDA-1	209.01	83.60	45.28
XDA-200	222.75	89.10	80.17

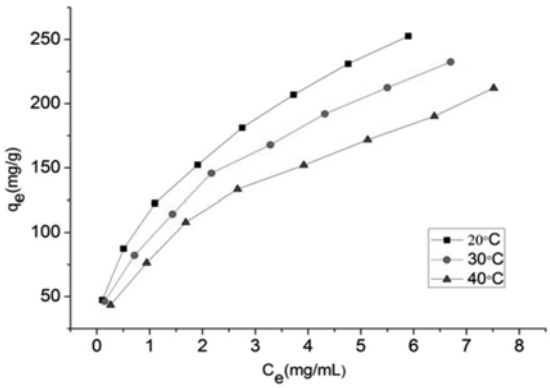

Fig. 2 — Adsorption isotherm of caffeine adsorbed on XDA-200 at different temperatures.

increase in the equilibrium concentration. However, higher temperature induces lower caffeine adsorption, indicating that the adsorption of caffeine onto XDA-200 is exothermic. As we know, at constant temperature, the caffeine adsorbed on the resin will be in equilibrium with the caffeine in solution.

Plotting $1/q_e$ versus $1/C_e$, $\ln q_e$ against $\ln C_e$, would produce a straight line. All the parameters calculated from the equations are shown in Table 3. As shown in Table 3, the Freundlich isotherm exhibited larger correlation coefficients, which indicated that the adsorption process for caffeine was a multimolecular layer adsorption and that the XDA-200 resin possessed a heterogeneous nature. The value of K_F decreased with increasing temperature, which further confirms the positive effect of low temperature on the adsorption of caffeine on XDA-200. In general, adsorption can occur easily when the 1/n value is between 0.1 and 0.5[19]. In this study, all values of 1/n were in the range of 0.1-0.5, which indicated that the adsorption of caffeine onto XDA-200 was favorable and could occur easily. These results are in agreement with the adsorption isotherms of caffeine onto XDA-200.

Adsorption thermodynamics on the selected resin

All thermodynamics parameters for the adsorption of caffeine onto XDA-200 are shown in Table 4.

As shown in Table 4, when the temperature was 293, 303 and 313K, ΔG was -11.64, -11.63 and -11.46 kJ/mol, respectively, all of which are negative, meaning that the adsorption process was spontaneous and feasible. Moreover, all ΔG values were less than 20 kJ/mol,which may indicate that the adsorption of caffeine onto XDA-200 occurred through physical adsorption[20].Additionally, the enthalpy value (ΔH) was negative, suggesting that the adsorption process was exothermic, and the results are in accordance with the trendin which the adsorption capacity decreased with increased temperature. In this study, the absolute value of enthalpy is 14.347 kJ/mol, which is in the range of the adsorption enthalpy related to hydrogen-bonding interactions (2-40kJ/mol). This mainly because the nitrogen atoms of caffeine act ashydrogen-bond acceptors and form hydrogen bonds with the hydrogen atoms of the hydroxyl groups of XDA-200. The positive ΔS for caffeine adsorption on XDA-200 suggested an increase in randomness or disorder at the solid-liquid interface during theadsorption process[21].The results indicate that the adsorption process may contain two steps:first, the desorptionof water and then the adsorption of caffeine.However, the molecular volume of caffeine is much larger than that of water, and thus many more water molecules should be desorbed before the same quantity of caffeinecan be adsorbed.

Adsorption kinetics on the selected resin

From Fig .3, we can clearly see that the adsorption capacity of caffeine onto XDA-200 rapidly increased

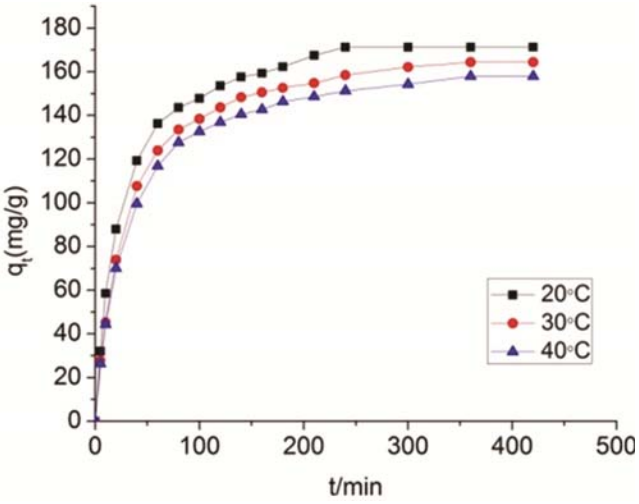

Fig. 3 — Adsorption kinetics curves of caffeine onto XDA-200.

Table 3 — Langmuir and Freundlich isotherm parameters of caffeine adsorbed on XDA-200 at 293, 303, and 313 K.

T(°C)	Langmuir				Freundlich			
20	Equation	R^2	K_L	q_{max}（mg/g）	Equation	R^2	K_F	1/n
	$C_e/q_e=0.00348C_e+0.0043$	0.9570	0.809	287.35	$\ln q_e=4.7790+0.4165\ln C_e$	0.9959	118.99	0.4165
30	$C_e/q_e=0.00369C_e+0.0058$	0.9577	0.636	271.00	$\ln q_e=4.6183+0.4298\ln C_e$	0.9907	101.32	0.4298
40	$C_e/q_e=0.00397C_e+0.0082$	0.9622	0.484	251.89	$\ln q_e=4.4019+0.4662\ln C_e$	0.9913	81.61	0.4662

Table 4 — Thermodynamics parameters for the adsorption of caffeine onto XDA-200.

T/K	K_F	△H/kJ·mol^{-1}	△G/kJ·mol-1	△S/J·mol^{-1}·K^{-1}
293	118.99		-11.64	88.70
303	101.32	-14.347	-11.63	85.75
313	81.61		-11.46	82.43

during the first 100 min, slowly increased until 240 min, and then reached a dynamic equilibrium. Therefore, the adsorption of caffeine onto XDA-200 may be a type of fast adsorption [22]. This is possibly because of the large number of vacant surface sites on XDA-200 initially available for adsorption, but the repulsive forces between the caffeine molecules on XDA-200 and those in the bulk phase make it difficult to occupy the remaining vacant surface sites[23]. As shown in Table 5, compared with the pseudo-first-order model, the pseudo-second-order model is more appropriate to describe the caffeine adsorption kinetics onto XDA-200, which exhibited higher correlation coefficient values. Moreover, the rate constant k_2 calculated in Table 5 provides an order of k_2(20 °C)> k_2(30 °C) > k_2(40 °C), suggesting that the adsorption process was exothermic, which is in accordance with the conclusions of the thermodynamics studies.

Figure 4 shows the relationship of q_t and $t^{1/2}$, and the multi-linearity of the plot suggests thatthe adsorption process might occur in three steps. The first sharper portion was due to the diffusion of caffeine from the solution to the external surface of XDA-200, and the adsorption system exhibited low mass transfer resistance in the bulk solution. However, the second step represents the gradual adsorption stage, in which intra-particle diffusion was the rate-limiting step, and the slower uptake might be attributed to the higher intra-particle transfer resistance. Finally, the third step is attributed to the final equilibrium stage [24]. Only when the plots of q_t versus $t^{1/2}$ pass the origin can intra-particle diffusion become the sole rate-limiting step. However, as shown in Fig. 4, the linear lines of the second and third regions did not pass through the origin, suggesting that there were multiple, simultaneous adsorption mechanisms controlling the rate of adsorption[25].

XPS and FTIR Analysis

XPS was used to monitor the surface electronic state of XDA-200 before and after adsorption. Figure 5 shows the survey scan of XDA-200 before and after the adsorption of caffeine. It can be seen that the electronic peak strengths of C(1s) and O(1s) were slightly enhanced, which can be attributed to the good adsorption of caffeine on the surface of XDA-200. A higher N(1s) electronic peak emerged after adsorption; however, there are no nitrogen elements in XDA-200, and thus this can be mainly attributed to the introduction of the nitrogen elements in caffeine.

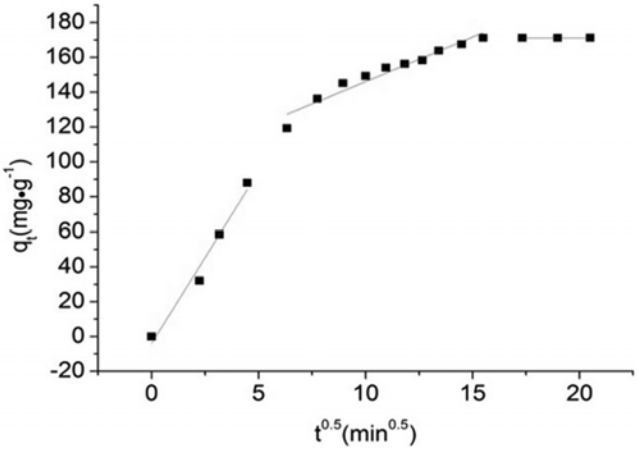

Fig. 4 — Intra-particle diffusion model plots for the adsorption of caffeine.

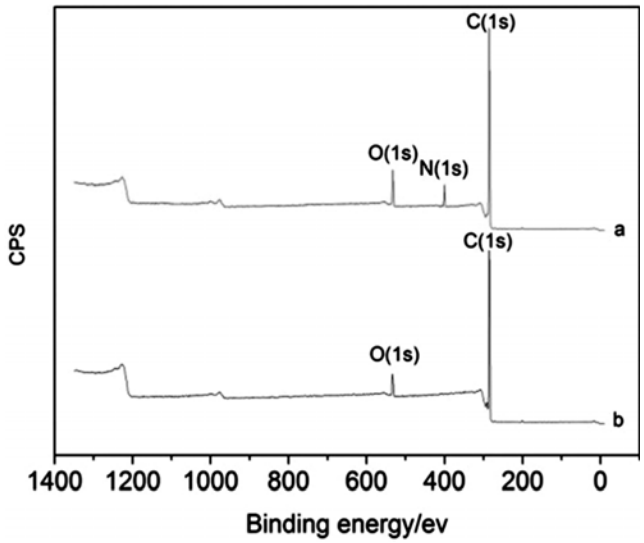

Fig. 5 — XPS survey scan of XDA-200: (a) after adsorption and (b) before adsorption.

Table 5 — inetics parameters of caffeine adsorbed onto XDA-200.

Temperature(°C)	Pseudo-first-order model			Pseudo-second-order model		
20 °C	q_e(mg/g)	k_1(g/mg·min)	R^2	q_e(mg/g)	K_2(g/mg·min$^{1/2}$)	R^2
	163.63	0.02337	0.9780	186.57	2.2739×10^{-4}	0.9987
30°C	155.79	0.02168	0.9870	175.43	2.1196×10^{-4}	0.9983
40°C	149.14	0.02282	0.9508	168.73	2.0785×10^{-4}	0.9969

The fine spectra of O(1s) before and after adsorption was studied. It can be seen that the bonding energy before adsorption is 532.58eV, while the bonding energy after adsorption is 533.08 eV, an increase of 0.5eV. It turned out that this chemical shift emerged after adsorption, and the higher bonding energy is due to the decreased outer electronic density of the O atom and the increased acting force between inner electrons and effective charge after adsorption.

In this study, FTIR was used to monitor the chemical changes of XDA-200 before and after adsorption. It is seen that some new peaks appeared after adsorption, where the peak at 1706 cm^{-1} was attributed to the stretching vibration of the carbonyl group. Moreover, the peak area at 2926 cm^{-1} had a slight decrease, which can be assigned to the adsorption of caffeine, which had very good coverage on the surface of the resin. XDA-200 is a styrene-divinylbenzene resin, and the infrared spectrum of XDA-200 has strong absorption peak at 3446.20 cm^{-1}, indicating that the resin contained many hydroxyl groups. However, the peak area at 2926 cm^{-1} had a slight increase after adsorption, which also verified the existence of the hydrogen-bonding interaction.

Conclusion

In this study, the adsorption characteristics of six commonly used macroporous resins were critically evaluated. XDA-200 showed a higher adsorption/desorption capacity and ratios than the other resins. The adsorption capacity of caffeine was 222.75 mg/g dry resin, and the adsorption and desorption ratios were 89.10% and 80.17%, respectively. The Freundlich isotherm model gives a good fit for the adsorption isotherm, indicating that the adsorption process for caffeine was a multimolecular layer adsorption. It was found that the experimental data fit best to the pseudo-second-order model, where multiple adsorption mechanisms were simultaneously controlling the rate of adsorption, and the adsorption process belonged to the fast adsorption type. The negative free energy (ΔG) implied that the adsorption was exothermic, and the positive entropy (ΔS) suggested that during the adsorption process the randomness of caffeine on XDA-200 was increased. The values of 1/n were in the range of 0.1- 0.5, which demonstrated that the adsorption of caffeine onto XDA-200 was favorable and could occur easily. The absolute value of enthalpy is 14.347 kJ/mol, which is in the range of the adsorption enthalpy related to hydrogen-bonding interactions. XPS and FTIR analyses showed that the bonding energy of O(1) increased by 0.5eV and that the peak area at 2926 cm^{-1} had a slight increase after adsorption, both of which demonstrate that hydrogen bonding between XDA-200 and caffeine occurred. In conclusion, the hydrogen-bonding interaction played an important role in the adsorption of caffeine, and compared with commonly used resins, XDA-200 may be more broadly applicable to the separation of caffeine because of its high adsorption capacity.

Acknowledgements

The authors express their thanks for the financial support from the Nature Science Foundation of Shandong Province, China (Project No.ZR2014BL027).

References

1 Utama-ang N, Phawatwiangnak K, Naruenartwongsakul S & Samakradhamrongthai R, *Food Chem*, 221(2017) 1733.
2 Unno K, Hara A, Nakagawa A,Iguchi K, Ohshio M, Morita A & Nakamura Y, *Phytomedicine*, 23(2016)1365.
3 Gramza-Michałowska A, Kobus-Cisowska J, Kmiecik D, Korczak J, Helak B, Dziedzic K & Górecka D, *Food Chem*, 211 (2016) 448.
4 Atik A, Harding R, Matteo R D, Kondos-Devcic D, Cheong J, Doyle L W & Tolcos M, *Neurotoxicology,* 58(2017)94.
5 Green J M, Olenick A, Eastep C & Winchester L, *Physiol Behav,* 169 (2017) 46.
6 Rd P C, Tomas A K, Taylor H A, Jacques P F & Kanarek R B, *Appetite,* 107 (2016) 69.
7 7Nawrot P, Jordan S, Eastwood J, Rotstein J, Hugenholtz A & Feeley M, *Food Addit Contama,* 20 (2003) 1.
8 Luszczki J J, Zuchora M, Sawicka K M, Kozińska J& Czuczwar S J, *Pharmacol Rep,* 70 (2015) 142.
9 Bermejo D V, Mendiola J A, Ibáñez E, Reglero G& Fornari T, *Food Bioprod Process,* 96 (2015) 106.
10 10Bermejo DV, IbáñezE, Reglero G & Fornari T, *J Supercri Fluid,* 107(2016)507.
11 Qi X L, Peng X, Huang Y Y, Li L, Wei Z F, Zu Y G & Fu Y J, *Ind Crop Prod,* 70 (2015) 142.
12 12Li KK, Zhou X L, Liu C L, Yang X R, Han X Q, Shi X G, Song X H, Ye C X & Ko C H, J *Chromatogr B*, 1011(2016)6.
13 ChenY, Zhang W J, ZhaoT, LiF, ZhangM, LiJ, ZouY, WangW, Cobbina S J, Wu X Y & Yang L Q, *Food Chem,*194 (2016) 712.
14 Huang J H, Huang K L, Liu S Q, Luo Q & Shi S Y, *J Colloid InterfSci,* 317 (2008) 434.
15 YangQ Y, Zhao M M & LinL Z, *Food Chem,* 194 (2016) 900.
16 16Zhuang M Z, Zhao M M, LinL Z, DongY, Chen H P, Feng M Y, Sun-Waterhouse D X & SuG W, *Food Chem,* 190 (2016) 338.

17 Liu B Y, Dong B T, Yuan X F, Kuang Q R, Zhao Q S, Yang M, Liu J & Zhao B, *J Chromatogr B*, 1008(2016)58.
18 18Xiong Q, Zhang Q, Zhang D, Shi Y, Jiang C & Shi X, *Food Chem*, 145 (2014) 1.
19 Li H J, Liu Y, Jin H Z, Liu S J, Fang S T, Wang C H & Xia C H, *J Chromatogr B*, 1007(2015)23.
20 20Du X, Yuan Q & Li Y, *Chem Eng Process*, 47 (2008) 1420.
21 21KuoC Y, *Desalination*, 249 (2009) 781.
22 22Wu X Y, Liu Y, Huo T, Chen Z B, Liu Y F, Di D L, Guo M & Zhao L, *Colloids Surf A: Physicochem Eng Aspects*, 487 (2015) 35.
23 23Charpe T W & Rathod V K, *Food Bioprod Process*, 93 (2015) 51.
24 24Zhao Q L, Gao Y C & Ye Z F, *Vacuum*, 95 (2013) 71.
25 Yang S F, Gao M L & Luo Z X, *Chem Eng J*, 256(2014) 39.